High-fidelity numerical investigation on structural integrity for SFR fuel cladding during design basis events

Seo Yoon Choia, Hyung Kyu Kimb, Jae-ho Jeonga†
aMechanical Engr. Gachon Uni., Seongnam-daero 1342, Sujeong-gu, Seongnam-si, Gyenggi-do
bKorea Atomic Energy Research Institute. 989-111 Daedeok-daero, Yuseoung-gu, Daejeon
jaeho.jeong@gachon.ac.kr

1. Introduction

Sodium-cooled fast reactors (SFRs) were developed in 1997 to reduce the amount of spent nuclear fuel and increase the uranium resource utilization. The Prototype Gen-IV Sodium-cooled Fast Reactor (PGSFR) design was developed in Korea in 2015 to achieve enhanced safety, efficient utilization of uranium resources, and to decrease the amount of waste. The specific design of the PGSFR, a pool-type SFR with thermal power of 392.2 MWt, is complete [1]. The basic design concepts of all the structures, systems, and components were determined and incorporated into the preliminary safety information document [2], which includes the basic design requirements and system descriptions and the results of the safety analysis for representative accident scenarios. The core outlet sodium temperature is designed to exceed 545 ℃ as the fuel/cladding is developed to secure 40% thermal efficiency [3].

The PGSFR fuel assembly operates at higher temperatures, that is at approximately 400–800 ℃, compared to the temperature of the water coolant in a pressurized water reactor (PWR) of around 320 ℃. Contrary to other reactors, the mechanical behavior of the PGSFR fuel assembly could be unexpected. Because the fuel rod is in direct contact with the core material, if it is damaged, an accident in which the core material is exposed may additionally occur. The structural stability was evaluated for other structures in the PGSFR, but not for the fuel rods. [4] Thus, it is necessary to assess the integrity of the fuel assembly at high temperatures by comparing the stress with the stress limit to demonstrate the structural safety in advance.

This paper presents a safety analysis and evaluation of the integrity of the structural materials used as the cladding and duct in a PGSFR. The evaluation method and criteria that apply to DBEs are presented.

2. Methodology and stress limit

2.1 Methodology

The procedure for evaluating the integrity of the fuel assembly components is shown in Fig. 1. First, the 217 wire-wrapped fuel rods and a hexagonal duct are modeled in detail for CFD and high-fidelity numerical structural analysis. Second, the PGSFR system is simulated using MARS-LMR code to determine the temperature of the cladding mid-wall. Third, CFD is performed to derive the temperature and pressure distribution of the fuel rods and the temperature of the duct during DBEs as well as under normal conditions. The temperature and pressure distributions of the fuel rods and duct are added to the input used for the structural analysis. Next, the structural analysis is performed to calculate the stress and strain of the cladding during DBEs using the ANSYS Mechanical software. Finally, the structural integrity is evaluated by comparing the stress and strain of the cladding with the stress limit and strain criteria.

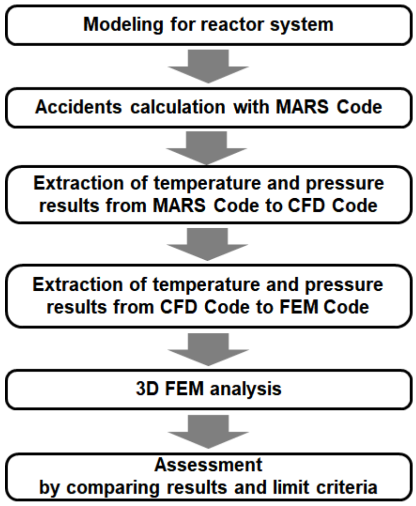

Fig. 1. Flow chart of system-related finite analysis.

2.2 Stress limits

Several researchers proposed new limits [5], and others, such as Briggs et al. (1995) and Puthiyavinayagam (2009), proposed new standards for a PGSFR [6,7], which are summarized in Table I. It should be noted that only the ultimate strength is used to determine the stress limits for the PGSFR fuel assembly. In the table, level A represents normal operation, level B is for anticipated operational occurrence (AOO) events, and level C events include design basis accident (DBA) class I and II events. Considering that σ_y and σ_u are functions of the temperature, the stress limit is also a function of the temperature. As a result, we prepared a master curve of the stress limits for each level, as given in Fig. 2. As the temperature increases, the stress limit decreases rapidly. Therefore, as the cladding temperature increases during DBEs, the thermal stress increases, but the limit is decreased.

Table I. Stress limit for PGSFR fuel assembly

Level	P_m	$P_m + P_b$	$P_m + P_b + Q$
A	$0.55\ \sigma_u$		$0.6\ \sigma_u$
B	$0.6\ \sigma_u$		$0.6\ \sigma_u$
C	$0.75\ \sigma_u$		$0.8\ \sigma_u$

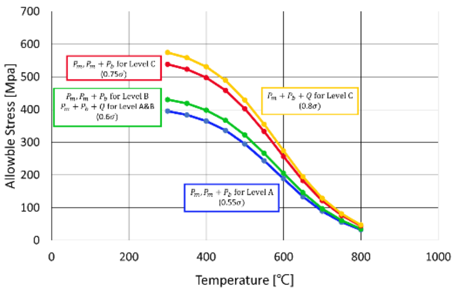

Fig. 2. Master curve for design.

3. Analysis of Design Basis Events

The temperature of the mid-wall of the fuel cladding is a major factor that determines the integrity of a fuel rod. Because increases in the temperature of the cladding mid-wall induce a high risk of damage to and breakage of the cladding, accidents which could possibly lead to damage and breakage of the cladding are chosen to evaluate the integrity of the fuel assembly components. Among the Transient over Power (TOP), Loss of Flow (LOF), and Loss of Heat Sink (LOHS) events, the critical and representative events are spurious Primary Heat Transfer System (PHTS), one pump seizure, and seismic reactivity insertion SSE (Safe Shutdown Earthquake) events, which is an AOO and a DBA Class II. For these three events, the temperature of the cladding mid-wall, power, and mass flow were calculated using the MARS LMR code. The temperature of the coolant, cladding, and fuel for the hottest nuclear fuel rod is conservatively calculated by considering hot channel factors. In spurious PHTS pump trip, the temperature of the cladding mid-wall reaches a maximum of 599.94 ℃ at 2.6 seconds. If the temperature is calculated considering HCFs, it reaches 636.27℃. This is a margin of more than 600 ℃ from the allowable standard temperature of 1,237 ℃. In one pump seizure. The temperature of the cladding reached a maximum of 655.32 ℃ at 1.75 sec. When HCFs are considered, the temperature rises to 715.45 ℃. This is a margin of more than 500 ℃ from the allowable standard temperature of 1,237 ℃. In seismic reactivity insertion SSE. The temperature of the cladding mid-wall reaches a maximum of 673.69 ℃ at 1.05 sec, and a maximum of 717.94 ℃ when HCFs are taken into account. This is a margin of more than 500 ℃ from the allowable standard temperature of 1,237 ℃.

4. Structural Analysis

4.1 Modeling

A structural analysis of the 217-pin fuel bundle and the hexagonal duct housing the fuel assembly comprising the fuel rod bundle of the PGSFR was carried out. The key design parameters of the 217-pin fuel bundle and hexagonal duct are provided in Table II and a cross-sectional view thereof is shown in Fig. 3. The wire is wound clockwise from the inlet with a pitch of 199.6 mm, as shown in Fig. 3. A cross-sectional drawing of the duct is shown in Fig. 4. The interior of the hexagonal duct is 126.36 mm wide and the exterior 132.36 mm, with a nominal thickness of 3mm. The fuel rods, wires, and duct are all manufactured from HT-9 materials. The fuel assembly was modeled using a three-dimensional finite element model of a fuel rod and duct.

Table II Geometric parameters of 217-pin fuel assembly

Geometric parameters	Value
Number of fuel fins	217
Pin diameter	7.4 mm
Pin pitch	8.436 mm
Pin axial length	2187.22 mm
Heated length	900 mm
Heat flux distribution	Non-Uniform
Tube flat-to-flat distance	126.36 mm
Wire spacer diameter	0.95 mm
Wire lead pitch	199.6 mm
Coolant	Sodium
Duct width (inner wall to wall)	126.36 mm
Duct thickness	3 mm
Duct length	0.1 m

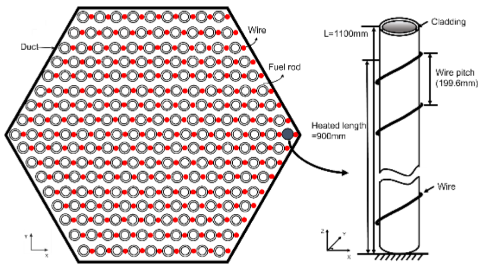

Fig. 3. Cross-sectional geometry of the fuel assembly and a single fuel pin with the wire winding.

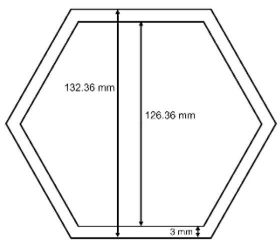

Fig. 4. Cross-sectional geometry of the hexagonal duct.

The fuel rods are mounted on a mounting rail. The mounting rail is positioned vertically within the hexagonal duct of the lower cap. The bottom of the model is clamped (including the duct, claddings, and wires). A gap for fuel expansion exists at the top end of the model. Three translational degrees of freedom (Dofs) and three rotational Dofs of the nodes at the upper side of the model are not constrained. The wire and fuel rod were assumed to be in contact. The model uses a normal hard and tangential frictionless contact property for the fuel rod and wire.

4.2 Modeling

The properties of the material required for the static-thermal structural analysis are the Young's modulus, Poisson's ratio, density, coefficient of thermal expansion, and thermal conductivity.

4.3 Modeling

Fig. 5 shows the temperature of the fuel rods at various positions in the vertical direction, and the pressure is plotted in Fig. 6. The temperature of the duct at various elevations from the base of the fuel rod is given in Fig. 7. The temperature increases whereas the pressure decreases as the elevation increases from the bottom.

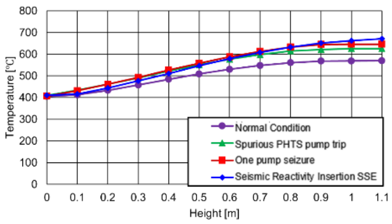

Fig. 5. Temperature distribution of fuel rods.

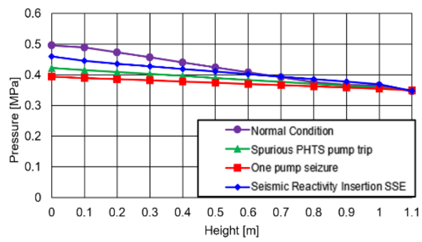

Fig. 6. Pressure distribution of fuel rods.

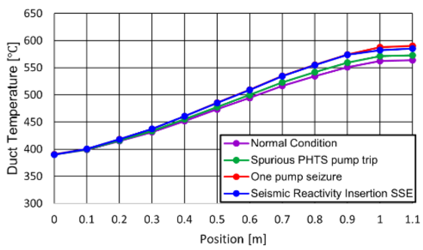

Fig. 7. Temperature distribution of duct.

5. Results

5.1 Stress assessment

The structural stability was evaluated by comparing the maximum stress during DBEs with the stress limits. The stress limit is obtained at the temperature where the maximum von Mises stress occurs. As shown in Fig. 8, the maximum stress occurs in the fuel rod rather than in the wire and duct. The stress is concentrated in the area of the fuel rod covered by the wire. The maximum stress occurs at top of the model. The stress at the top of the center of the fuel rod below the wire is compared with the stress limit during DBEs. Table III summarizes the maximum stress of the membrane and the sum of membrane and bending stress, in addition to the total stress, stress limit, and safety margins during DBEs.

Membrane stress and bending stress, which are primary stresses, are generated by pressure and exclude thermal stress. The membrane stress was confirmed to differ insignificantly because the pressure acting on the fuel rods in each event is similar. The total stress generated is the highest in the seismic reactivity insertion SSE accident during operation at the highest temperature. This confirms that the stress does not induce the breakage of the cladding and the safety margin of 40% or more is sufficient. The result of evaluating the stress in two representative cases corresponding to DBA Class II led to the conclusion that all of the parameters enable safe operation.

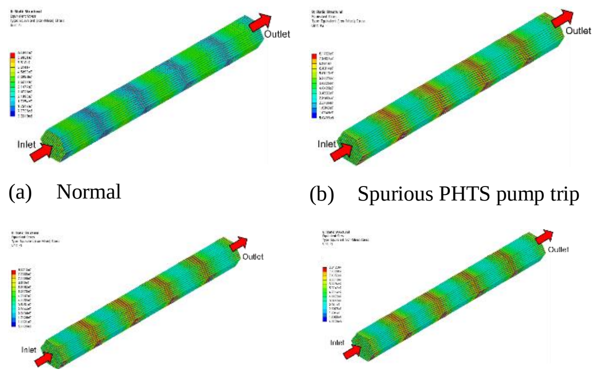

(a) Normal
(b) Spurious PHTS pump trip
(c) One pump seizure
(d) Seismic reactivity insertion SSE

Fig. 8. Typical view of the stress concentration in the fuel assembly during normal operation and accident events.

Table III Stress results

Condition		P_m	$P_m + P_b$	$P_m + P_b + Q$
Normal	Minimum stress limit [MPa]	222 (<0.55$\boldsymbol{\sigma_u}$ at 569 ℃)		242.3 (<0.6$\boldsymbol{\sigma_u}$ at 569 ℃)
	Maximum Stress [MPa]	36.62	46.21	64.66
	Safety Margin [%]	83.5	79.2	72
Spurious PHTS pump trip	Minimum stress limit [MPa]	173 (<0.6$\boldsymbol{\sigma_u}$ at 626 ℃)		
	Maximum Stress [MPa]	36.57	45.81	81.7
	Safety Margin [%]	78.9	73.5	52.8

One pump seizure	Minimum stress limit [MPa]	188 (<0.75$\boldsymbol{\sigma_u}$ at 646 ℃)		230.7 (<0.8$\boldsymbol{\sigma_u}$ at 646 ℃)
	Maximum Stress [MPa]	36.5	45.4	85.5
	Safety Margin [%]	74.5	73.6	62.9
Seismic reactivity insertion SSE	Minimum stress limit [MPa]	155.5 (<0.75$\boldsymbol{\sigma_u}$ at 670.5 ℃)		166 (<0.8$\boldsymbol{\sigma_u}$ at 670.5 ℃)
	Maximum Stress [MPa]	38.05	49.73	87
	Safety Margin [%]	69.1	68	47.6

5.2 Strain assessment

The main parameters that express the fuel design limit are the cumulative damage fraction (CDF) and strain. The allowable nuclear fuel design limit for an SFR is applied at a strain rate of 1% for AOO and DBA Class I&II accidents. The strain in the cladding for each type of accident is shown in Fig. 9. In all cases, the maximum strain experienced by the cladding is lower than the limit of 1%. This means that cracking of the oxide film is not induced. Radial cracking of the oxide film would cause stress concentration at the crack tip, which would act as an initiation point for cracks in the cladding. This has the potential to ultimately cause the cladding to rupture. Since the strain is much lower than the limit, the failure risk of the cladding is concluded to be low. [8]

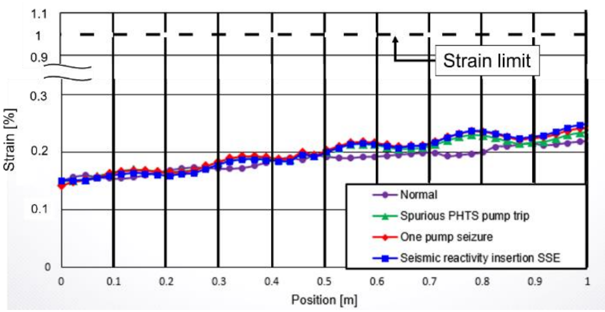

Fig. 9. Strain results.

6. Conclusions

In this study, the integrity of PGSFR fuel assembly components was assessed by conducting a structural analysis for DBEs, spurious PHTS pump trip, single-pump seizure in an LOF accident, and seismic reactivity insertion SSE of a TOP accident, as well as during normal operation. These events are AOO and DBA Class II events.

- The temperature of the PGSFR fuel assembly was confirmed to remain lower than 1237 ℃ as a result of the conservative temperature considering the hot channel factors.
- The stress experienced by the PGSFR fuel assembly is shown to not compromise the safety with minimum and maximum safety margins of 47% and 72%, respectively, during normal operation and accident events.
- The strain of the cladding is confirmed to be much lower than the specified 1%.

Based on these analysis results, it is concluded that the structural integrity of the PGSFR fuel assembly is guaranteed during DBEs as well as during normal operation.

This study involved a static structural analysis of the fuel assembly components of a PGSFR. As a follow-up study, we intend to proceed with fatigue analysis.

REFERENCES

[1] K. L. Lee., K.-S. Ha., J.H. Jeong., C.-W. Choi., T. Jeong, S. J. Ahn., S. W. Lee., W.-P. Chang, S. H. Kang, J. Yoo, A Preliminary Safety Analysis for the Prototype Gen IV Sodium-Cooled Fast Reactor, Nuclear Eng. Technol. 48 1071-1082, 2016

[2] System Description of Prototype Gen-IV Sodium-cooled Fast Reactor, SFR-000-SP-403e001, Korea Atomic Energy Research Institute, 2015.

[3] J. Yoo, J. Chang, J.-Y. Lim, J.-S. Cheon, T.-H. Lee, S. K. Kim, K. L. Lee, H.-K. Joo, Overall system description and safety characteristics of prototype Gen IV sodium cooled fast reactor in Korea, Nuclear Eng. Technol. 48 1059-10704, 2016

[4] K.H. Yoon, H.-K. Kim, H.S Lee, J.S. Cheon, Component design and accident analysis fuel assembly for prototype GEN-IV sodium-cooled fast reactor, 2018, Nuclear Eng. Design 340, pp. 133-145, 2018

[5] J.-H. Kim, J.-W. Lee, K.-H. Kim, C.-B. Lee, Preliminary Study on the Fabrication of Particulate Fuel through Pressureless Sintering Process, Sci. Technol. Nucl. Install, 3717361, 2016

[6] ASME Section III, 2013, In: Division 5 Article HGB-3000, pp. 123-138

[7] RCC-MRx, 2012 Edition with 2013 1st Addendum. SECTION III (Rules for Mechanical Components of Nuclear Installation) – TOME 1 (Design and Construction Rules) – SUBSECTION B (Class NIRx Reactor Components, Its Auxiliary Systems and Supports) – RB 3000 (Design), & - SUBSECTION Z (Technical Appendices)

[8] S.-S. Kang, S.-H. Kim, Y.-K. Jung, C.-Y. Yang, I.-G. Kim, Y.-H. Choi, H.-J. Kim, M.-W. Kim, B.-H. Rho, Study on the Standard Establishment for the Integrity Assessment of Nuclear Fuel Cladding Materials, Technical Report KAERI, 2007